



**HAL**  
open science

# Bacterial ice nuclei impact cloud lifetime and radiative properties and reduce atmospheric heat loss in the BRAMS simulation model

Tassio S Costa, Fábio L. T. Gonçalves, Marcia A Yamasoe, Jorge A Martins,  
Cindy E. Morris

## ► To cite this version:

Tassio S Costa, Fábio L. T. Gonçalves, Marcia A Yamasoe, Jorge A Martins, Cindy E. Morris. Bacterial ice nuclei impact cloud lifetime and radiative properties and reduce atmospheric heat loss in the BRAMS simulation model. *Environmental Research Letters*, 2014, 9 (8), pp.084020. 10.1088/1748-9326/9/8/084020 . hal-02632404

**HAL Id: hal-02632404**

**<https://hal.inrae.fr/hal-02632404>**

Submitted on 27 May 2020

**HAL** is a multi-disciplinary open access archive for the deposit and dissemination of scientific research documents, whether they are published or not. The documents may come from teaching and research institutions in France or abroad, or from public or private research centers.

L'archive ouverte pluridisciplinaire **HAL**, est destinée au dépôt et à la diffusion de documents scientifiques de niveau recherche, publiés ou non, émanant des établissements d'enseignement et de recherche français ou étrangers, des laboratoires publics ou privés.

## Bacterial ice nuclei impact cloud lifetime and radiative properties and reduce atmospheric heat loss in the BRAMS simulation model

This content has been downloaded from IOPscience. Please scroll down to see the full text.

2014 Environ. Res. Lett. 9 084020

(<http://iopscience.iop.org/1748-9326/9/8/084020>)

View [the table of contents for this issue](#), or go to the [journal homepage](#) for more

Download details:

IP Address: 147.100.71.242

This content was downloaded on 16/10/2014 at 10:54

Please note that [terms and conditions apply](#).

# Bacterial ice nuclei impact cloud lifetime and radiative properties and reduce atmospheric heat loss in the BRAMS simulation model

Tassio S Costa<sup>1</sup>, Fábio L T Gonçalves<sup>1</sup>, Marcia A Yamasoe<sup>1</sup>,  
Jorge A Martins<sup>2</sup> and Cindy E Morris<sup>3</sup>

<sup>1</sup>Department of Atmospheric Sciences, IAG/USP/Brazil Rua do Matão 1226, São Paulo 05508090, SP, Brazil

<sup>2</sup>Universidade Tecnológica Federal do Paraná, 86036-370, Londrina, PR, Brazil

<sup>3</sup>INRA, UR407 Pathologie Végétale, F-84143 Montfavet, France

E-mail: [fabio.goncalves@iag.usp.br](mailto:fabio.goncalves@iag.usp.br)

Received 21 February 2014, revised 7 July 2014

Accepted for publication 21 July 2014

Published 26 August 2014

## Abstract

This study examines the effect of the bacterial species *Pseudomonas syringae* acting as ice nuclei (IN) on cloud properties to understand its impact on local radiative budget and heating rates. These bacteria may become active IN at temperatures as warm as  $-2$  °C. Numerical simulations were developed using the Brazilian Regional Atmospheric Model System (BRAMS). To investigate the isolated effect of bacterial IN, four scenarios were created considering only homogeneous and bacterial ice nucleation, with 1, 10 and 100 IN per cubic meter of cloud volume and one with no bacteria. Moreover, two other scenarios were generated: the BRAMS default parameterization and its combination with bacterial IN. The model reproduced a strong convective cell over São Paulo on 3 March 2003. Results showed that bacterial IN may change cloud evolution as well as its microphysical properties, which in turn influence cloud radiative properties. For example, the reflected shortwave irradiance over an averaged domain in a scenario considering bacterial IN added to the BRAMS default parameterization was 14% lower than if bacteria were not considered. Heating rates can also be impacted, especially due to differences in cloud lifetime. Results suggest that the omission of bacterial IN in numerical models, including global cloud models, could neglect relevant ice nucleation processes that potentially influence cloud radiative properties.

Keywords: biological ice nuclei, cloud radiative properties, numerical modeling

## 1. Introduction

Over the past 5 years there has been a surge of research on the impact of atmospheric ice nuclei (IN) of biological origin on physical and chemical processes in clouds. Recent measurements by Pratt *et al* (2009) and Prenni *et al* (2009), for example, provide support for a relevant role of biological particles in ice nucleation processes. Vaitilingom *et al* (2013) have shown the potential of microorganisms—via their

metabolic properties—to reduce the oxidative capacity of clouds.

Considerable evidence is also mounting for the role of ice nucleation active (INA) bacteria and fungi in physical processes leading to rain and snowfall, and in particular under relatively warm conditions where mineral IN are inefficient in these processes. The reciprocal response of these INA microorganisms and of their sources to the resulting precipitation is likely to lead to a feedback process that reinforces both the plant and microbial populations involved (Morris *et al* 2014). Because of the ice generated in the events preceding precipitation, the potential impact of INA microorganisms on electrification of clouds and on the number of



Content from this work may be used under the terms of the Creative Commons Attribution 3.0 licence. Any further distribution of this work must maintain attribution to the author(s) and the title of the work, journal citation and DOI.

lightning flashes has also been investigated (Gonçalves *et al* 2012). The scale of the impact of these phenomena has been debated. Recent studies considering microbial IN showed that under typical microbial concentrations no significant effect on precipitation was found on a global scale (Hoose *et al* 2010, Sesartic *et al* 2012), whereas there is evidence for an effect on a regional scale (Spracklen and Heald 2013).

One of the last frontiers to be explored concerning the impact of biological aerosols on cloud processes involves the effects on radiative properties. Considering their potential for acting as IN, biological aerosols, in the same way as inert aerosols, can interact with radiation by processes of emission, absorption and reflection/scattering (Morris *et al* 2011). In this context, cloud properties are very important to the energy balance of the terrestrial atmosphere, holding infrared radiation emitted by the surface as well as partially scattering and reflecting solar radiation through their high albedo. But, despite their importance, cloud processes are still some of the least understood in the atmospheric sciences and are not adequately simulated in global climate change projections (Forster *et al* 2007).

The impact of marine aerosols as IN for cloud processes has also been investigated (Knopf *et al* 2011, Bigg 1973). More recently, Yun and Penner (2013) have used a global circulation model coupled with an aerosol transport model to show that the omission of ice nucleation due to marine organic aerosols on the simulations may cause a bias in the present-day cloud radiative forcing, due to an under-prediction of the ice water path in the Southern Hemisphere.

The main goal of this work is to investigate the effect of bacterial IN on the local radiative irradiances and heating rates due to their interactions with clouds. This study complements the analysis initiated by Gonçalves *et al* (2012) where numerical simulations with distinct concentrations of IN for a typical summer day at São Paulo city were conducted using Brazilian Regional Atmospheric Model System (BRAMS). Their purpose was to investigate the impact of ice nucleation-active-bacteria on the amount of rainfall, cloud electricity, particularly flash rates. In this present work we have used the cloud properties from BRAMS as input in a radiative transfer code. Details on the cloud model can be found in Gonçalves *et al* (2012).

## 2. Methodology

The cloud properties used as input for the radiative transfer simulations were obtained from the BRAMS cloud model fed with data from a radiosonde released in São Paulo on 3 March 2003. A strong convective cell was presented on that day, typical of summertime in São Paulo. As aforementioned, the cloud model used here corresponds to that used by Gonçalves *et al* (2012) and is briefly described below.

### 2.1. BRAMS model

A low level forcing, following Gonçalves *et al* (2008), was applied to induce the development of a convective cell. Temperature and humidity profiles of a radiosonde released in São Paulo (23.63° S; 46.57° W) were used to initiate the model. The domain comprised an area of 60 km × 60 km, with 500 m horizontal resolution, and 20 km in the vertical with a logarithmically varying resolution. The output time step was 2 min, but the simulation time step was 1 s. The total simulated interval was 3 h. The simulations were satisfactorily comparable to radar data retrieved during the convective cell development (Gonçalves *et al* 2012).

In terms of cloud formation mechanisms, BRAMS uses a set of microphysical parameterizations in order to represent the seven categories of liquid and solid water as follow: cloud droplets, rain, pristine ice, snow, aggregates, graupel and hail. Basically, the BRAMS microphysical parameterization predicts mixing ratios and number concentrations for each category. The hydrometeors in each category are assumed to be distributed by a generalized gamma function. Although the activation of a category is a user choice, all seven water categories were activated in the simulations performed in this study. The several microphysical processes used by the model include: vapor/heat diffusion, collision/coalescence (including self-collection and riming of cloud droplets by ice categories), melting, freezing, heterogeneous nucleation of ice, homogeneous nucleation of cloud droplets/haze into ice crystals, secondary production of ice and shedding of liquid water by hail, as well as collisional breakup and sedimentation. The parameterizations of specific cloud-rain microphysical processes represented in BRAMS can be found in a number of other studies such as: Flatau *et al* (1989), Pielke *et al* (1992), Walko *et al* (1995) and Meyers *et al* (1997). Most of the microphysical processes are also discussed by Khain *et al* (2000) in a review of the state-of-the-art numerical modeling of cloud microphysics. Considering the main goal of this study, only the processes associated with CCN and IN activation will be described thoroughly next.

For the CCN activation mechanism, the BRAMS model uses information from a pre-computed table of CCN concentration. The table is built based on atmospheric parameters and two empirical CCN activation parameters as described in Twomey and Wojciechowski (1969). Essentially, during each time step of the simulation, supersaturation increases as a result of vertical advection and the number of cloud droplets is defined by accessing the pre-computed table. The CCN field is initialized from the concentration specified by the user but evolves in time thereafter. In the present study, the CCN concentration was set to 300 cm<sup>-3</sup> throughout the simulation. Although there is no removal process associated with CCN, transport by advection and diffusion can modify CCN concentration at any grid point.

A variety of physical mechanisms promoting nucleation of pristine ice crystals is parameterized in the model. Deposition nucleation may occur at ambient temperatures below -5 °C since ambient water vapor mixing ratio exceeds saturation over ice. Condensation-freezing nucleation occurs

**Table 1.** Summary of ice nucleation modes considered for each scenario. Other processes refer to deposition, condensation and freezing, and contact and freezing.

	S1	S2	S3	S4	S5	S6
Homogeneous	Yes	Yes	Yes	Yes	Yes	Yes
Homogeneous + other processes	No	No	No	No	Yes	Yes
Bacterial IN	No	Yes w. $1 \text{ m}^{-3}$	Yes w. $10 \text{ m}^{-3}$	Yes w. $100 \text{ m}^{-3}$	No	Yes w. $100 \text{ m}^{-3}$

at temperatures below  $-2 \text{ }^\circ\text{C}$  and requires supersaturation with respect to liquid water. Although the two processes are permitted at temperatures below these thresholds, the actual number of nucleated crystals will be a function of the environmental conditions, but time independent. Deposition nucleation and condensation-freezing are represented by a single empirically-based parameterization described by Meyers *et al* (1992). Contact freezing nucleation occurs by the contact between an IN and a super-cooled cloud water droplet. Three basic phenomena will promote this process: vapor mass flux toward the growing droplet carries IN (Diffusiophoresis); a gradient of temperature around evaporating droplets push IN to the droplets (Thermophoresis); IN can collide with droplets due to random collisions with air molecules (Brownian motion). The number of IN available for contact freezing nucleation is a function of temperature. The parameterization of the number of crystals, produced by contact freezing nucleation, is described in Cotton *et al* (1986) and Meyers *et al* (1992). Homogeneous nucleation of supercooled water in BRAMS involves activated and unactivated cloud droplets. In the first case, the process is based on empirical results of DeMott *et al* (1994), where the number of cloud droplets freezing in a time-step is dependent on the size of the droplet and temperature in the range  $-30 \text{ }^\circ\text{C}$  to  $-50 \text{ }^\circ\text{C}$ . For colder temperatures, the value  $-50 \text{ }^\circ\text{C}$  is applied. For the unactivated droplets (haze particles) the fraction of particles homogeneously freezing in a time-step is dependent on the temperature, humidity and type of solute. The solute is assumed to be ammonium sulfate. The secondary production of ice crystals follows the Hallett-Mossop ice multiplication theory (Hallett and Mossop 1974, Mossop 1976), with additional modifications proposed by Cotton *et al* (1986, 2003). According to the parameterization included in BRAMS, the rate of crystal production is a function of the concentration of cloud droplets smaller than  $12 \text{ }\mu\text{m}$  and larger than  $24 \text{ }\mu\text{m}$  in radius and rime accreted on graupel particles in the range  $-8 \text{ }^\circ\text{C}$  to  $-3 \text{ }^\circ\text{C}$ . Empirical results reported by Hallett and Mossop (1974) showed that approximately 350 ice splinters are produced for every milligram of rime which are accreted on graupel particles at  $-5 \text{ }^\circ\text{C}$ .

Once an ice nucleation process is activated and produces the first nuclei, they will be categorized as pristine ice. The pristine ice category involves relatively small crystals, while larger ice crystals are categorized as snow. Once nucleated, pristine ice continues growing by vapor deposition, which is the only growth process permitted for the category. The snow category can grow by vapor deposition and riming. A bimodal representation of ice crystals is assumed for the two categories. Although pristine ice is the smallest of the solid

categories, it falls and the only category assumed small enough to not fall is cloud droplets. In addition, pristine ice and snow are classified as one of five ice crystal types depending on cloud temperature and humidity: columns, needles, hexagonal plates, dendrites or rosettes. The collision and coalescence of pristine ice and snow will form aggregates, which are formed with low amount of riming. Graupel is formed by a relatively high amount of riming and partial melting of ice associated to the pristine ice, snow and aggregate categories (low percentage of liquid water). Hail is assumed to be formed by freezing of rain drops or by riming or partial melting of graupel. In this case, note that a snow or aggregate suffering gradual melting first converts to graupel, then to hail, and finally to rain. Additional information about the categories represented in BRAMS can be found in Walko *et al* (1995).

### 2.2. Ice nucleation modeling

The experiment consisted of six distinct scenarios, including bacteria acting as IN with different vertical profiles, referred to as S1, S2, S3, S4, S5 and S6, based on Gonçalves *et al* (2012). S1 considered only homogeneous nucleation by DeMott *et al* (1994), in the temperature range from  $-30 \text{ }^\circ\text{C}$  to  $-50 \text{ }^\circ\text{C}$  (the value at  $-50 \text{ }^\circ\text{C}$  was applied to colder temperatures). Then in order to investigate the effect of bacterial IN concentrations, a load of 1, 10 and 100 bacterial IN per cubic meter of cloud volume was added to scenarios S2, S3 and S4, respectively, in addition to homogenous nuclei.

S5 corresponds to the BRAMS default parameterization, which considers ice nucleation through the following modes: homogeneous (as in S1), deposition and condensation-freezing (Meyers *et al* 1997), and contact freezing (Cotton *et al* 1986). This parameterization accepts ice nucleation only at temperatures colder than  $-8 \text{ }^\circ\text{C}$ , in contrast to that due to bacterial IN (S2, S3, and S4), which allows nucleation at temperatures as warm as  $-2 \text{ }^\circ\text{C}$ . Finally, the scenario S6—a combination of S4 and S5—was generated in order to assess the effect of omitting ice nucleation due to bacterial IN in BRAMS default runs. Table 1 summarizes the ice nucleation modeling.

### 2.3. Cloud radiative properties

Radiative transfer simulations were performed using the libRadtran (Mayer and Kylling 2005) atmospheric radiative transfer code, version 1.7. The required input of cloud properties are the vertical profiles of the hydrometeor effective radius and content, in liquid and ice thermodynamic phases. These input parameters were obtained from the BRAMS

cloud model considering the different bacterial loads previously described. The hydrometeor size distributions from BRAMS were converted into effective radius assuming a Gamma Distribution and a shape-parameter of 2 for droplets and pristine crystals and 1 for the remaining hydrometeor classes.

The cloud microphysical properties provided were subsequently converted into optical properties. For this purpose, the parameterization by Hu and Stamnes (1993) was used for water droplets, and by Yang *et al* (2005) for ice crystals. Snow, pristine and aggregates were considered in the radiative transfer simulations. The remaining hydrometeors (rain, hail and graupel) exhibited negligible contribution in the radiative transfer simulations when compared to the former. The droxtal habit from Yang *et al* (2005) was chosen for the ice hydrometeors.

Vertical profiles of air temperature and density from BRAMS were incorporated into the simulations from 1000 hPa until 50 hPa. The tropical atmosphere from the libRadtran library was then used to extend them to the top of the atmosphere. Urban surface albedo was selected from the IGBP library (Loveland and Belward 1997). Gaseous absorption was taken into account through the correlated *k* approximation by Kato *et al* (1999) in the shortwave spectrum and by Fu & Liou (1992) in the longwave spectral region.

The radiative transfer equation was solved using the Two Stream method as proposed by Kylling *et al* (1995). Overcast clouds were assumed for the simulations. The shortwave spectrum refers to the wavelength range of 280–3000 nm, and the longwave spectrum to the wavelength range of 3000–100 000 nm.

For each scenario, the mean and respective standard deviation irradiance values at the top and bottom of the atmosphere were estimated for both the shortwave and longwave spectral regions. To do so, horizontal grid points over 5 km within the cell center and a time range from 20 to 80 min were considered.

#### 2.4. Statistical tests

In order to verify if the radiation budget was affected by the distinct bacterial IN concentrations, a statistical test for the differences of the mean was applied, considering the null hypothesis that the two underlying means are equal (Wilks 2006):

$$z = \frac{\bar{x}_1 - \bar{x}_2}{\left[ \frac{s_1^2}{n_1} + \frac{s_2^2}{n_2} \right]^{\frac{1}{2}}},$$

where  $\bar{x}_1$ ,  $s_1^2$  and  $n_1$  are respectively the mean, variance and number of data points used to estimate the mean of irradiance for a given scenario, while  $\bar{x}_2$ ,  $s_2^2$  and  $n_2$  refer to the same parameters but for the scenario taken as reference. According to Wilks (2006), for moderately large samples ( $n > 100$ ) the sampling distribution of *z* is close to the Gaussian, due to the Central Limit Theorem. Moreover, if the absolute value of *z* is

equal or larger than 2.0, the two means can be considered statistically different at the 5% significance level.

### 3. Results

Radiative transfer is sensitive to cloud microphysical properties—such as hydrometeor size distribution, liquid/ice water content and crystal shape—as well as to macrophysical properties (e.g., cloud vertical and horizontal extent). The hydrometeor concentration distributions were given Gonçalves *et al* (2012) in more details. These concentration distributions can also affect indirectly and directly size distributions, due complex interactions where cloud height, temperature profiles, vapor profiles and hydrometeor competitions are included. Given that the activation of aerosol particles as cloud condensation nuclei or IN can play a decisive role in the cloud development and structure, an increased concentration of bacteria may hence eventually influence the radiative quantities. The following results compare the irradiances and radiative heating rates in the shortwave and longwave spectra for the six distinct scenarios previously described.

If, besides homogeneous nucleation, only ice nucleation due to bacterial concentrations is considered (scenarios S2, S3 and S4), it can be observed in figures 1 and 2 that an increase in the concentration of bacteria affects both cloud spatial extent and lifetime when compared to S1. The highest shortwave albedo is predicted for S5 (figure 1). When ice nucleation due to bacteria is added to the BRAMS default parameterization (S6), the reflection of solar radiation is notably decreased. This may be attributed to an increase in ice crystal size, as discussed below.

Because cloud optical depth is a function directly dependent on particle concentration and size distribution, different particle effective radii are expected to produce different results of radiative transfer through cloud layers. For a fixed cloud water concentration, a cloud composed of smaller particles is more optically active than if it was composed of larger particles. Table 2 shows the effective radius of ice hydrometeors averaged over 5 km within the cell center and from 20 to 80 min of simulation. Relative differences comparing the scenarios with the BRAMS default (S5) are also presented in table 2. Large differences among the scenarios are observed. When compared to S1, the injection of bacteria (S2, S3 and S4) tended to reduce the mean effective radius, which can be explained by the fact that an increased concentration of IN increases the cloud particle number concentration and consequently reduces the mean effective radius. This was however a nonmonotonic behavior, since an increase in the mean effective radius is observed from S2 and S3 for every ice hydrometeor class. S5 exhibited the smallest ice particles in average, which implies higher optical activity, but when bacterial IN were added to that simulation, the effective radius of ice hydrometeors was increased (S6).

Figure 3 displays the ice water path of snow and pristine ice crystals for each scenario as a function of time and distance from cell center. Pristine crystals dominate in S5, while

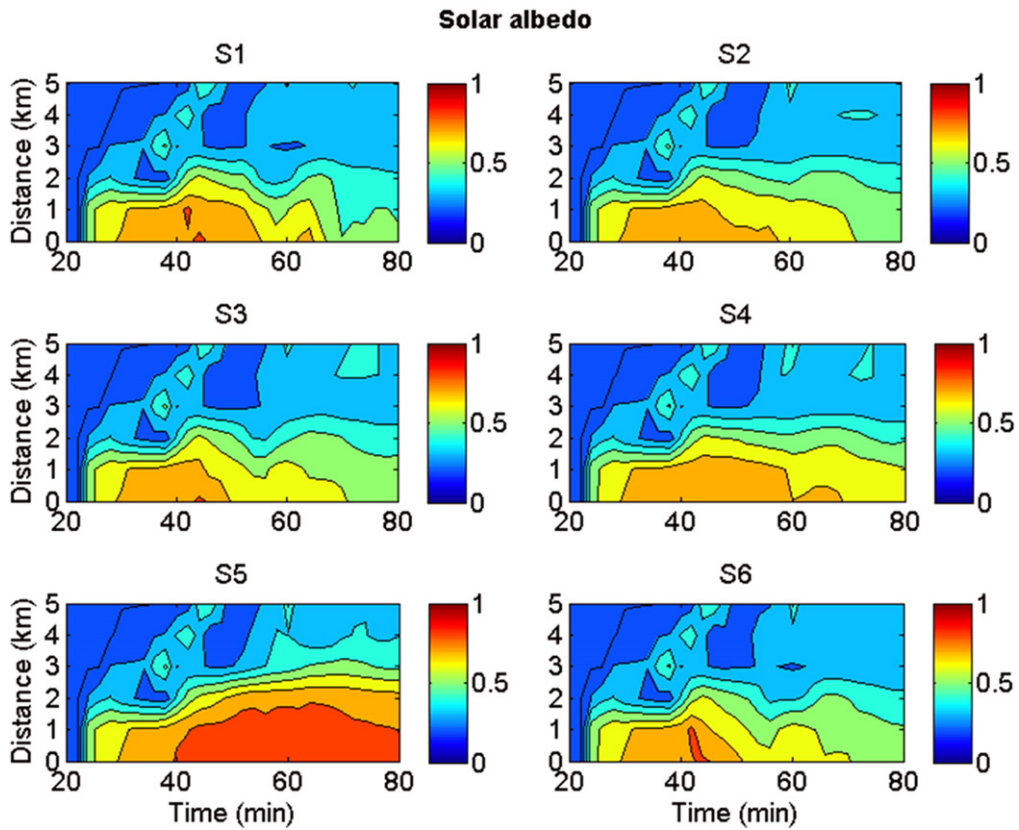


**Figure 1** Shortwave albedo at the top of the atmosphere for each scenario. The vertical scale represents the horizontal extension of the cloud from its center and the horizontal scale indicates the time evolution of the cloud.

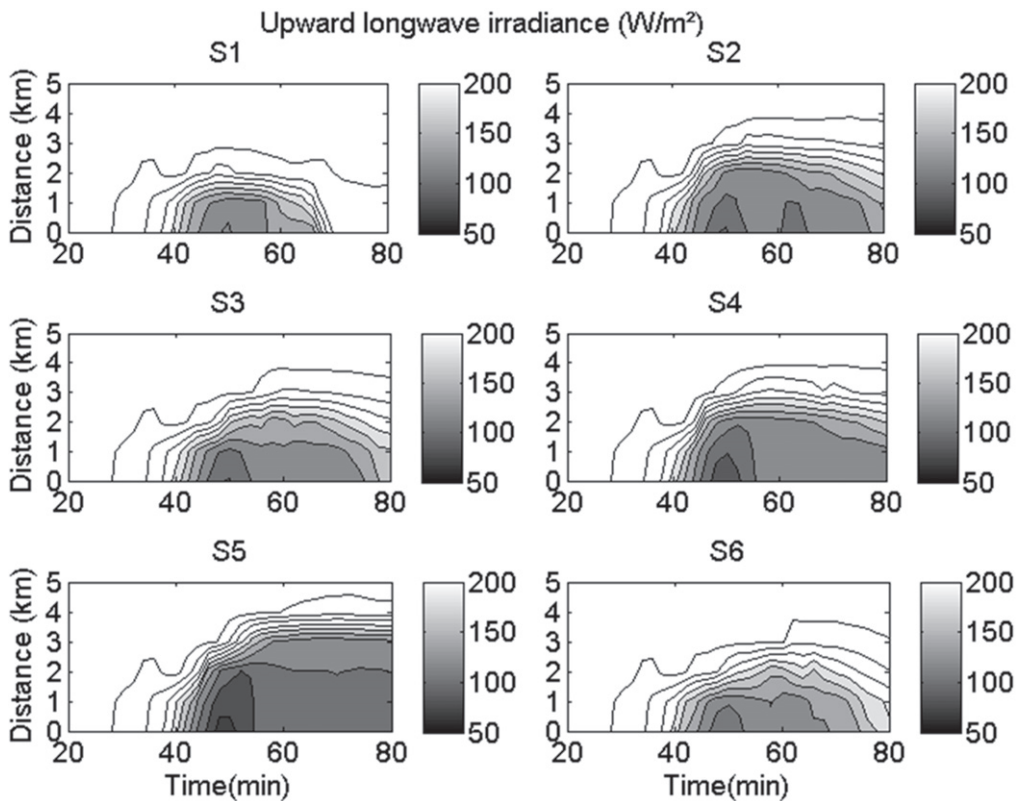


**Figure 2** Emitted longwave irradiance at the top of the atmosphere for each scenario. The vertical scale represents the horizontal extension of the cloud from its center and the horizontal scale indicates the time evolution of the cloud.

**Table 2.** Effective radius ( $\mu\text{m}$ ) of the hydrometeors considered in the simulations. Values were averaged over a domain of 5 km within the cell center and from 20 thru 80 min of the simulations. The relative differences (%) compared to the BRAMS default are shown in brackets.

	S1	S2	S3	S4	S5	S6
Droplet	$26.73 \pm 0.14$ (-4.0%)	$27.34 \pm 0.05$ (-1.8%)	$27.103 \pm 0.021$ (-2.6%)	$27.57 \pm 0.27$ (-0.9%)	$27.83 \pm 0.32$	$27.09 \pm 0.04$ (-2.7%)
Pristine	$81.27 \pm 0.53$ (247%)	$71.332 \pm 0.020$ (204%)	$75.6 \pm 1.5$ (222%)	$54.04 \pm 0.70$ (130%)	$23.45 \pm 0.28$	$81.73 \pm 1.4$ (248%)
Snow	$204.6 \pm 2.7$ (359%)	$92 \pm 22$ (108%)	$115.6 \pm 2.3$ (160%)	$107.0 \pm 2.0$ (140%)	$45 \pm 30$	$134.4 \pm 3.2$ (202%)
Aggregates	$844 \pm 21$ (1083%)	$204.6 \pm 1.9$ (187%)	$254.7 \pm 2.4$ (257%)	$146.90 \pm 0.14$ (106%)	$71.35 \pm 0.12$	$284.5 \pm 1.8$ (299%)

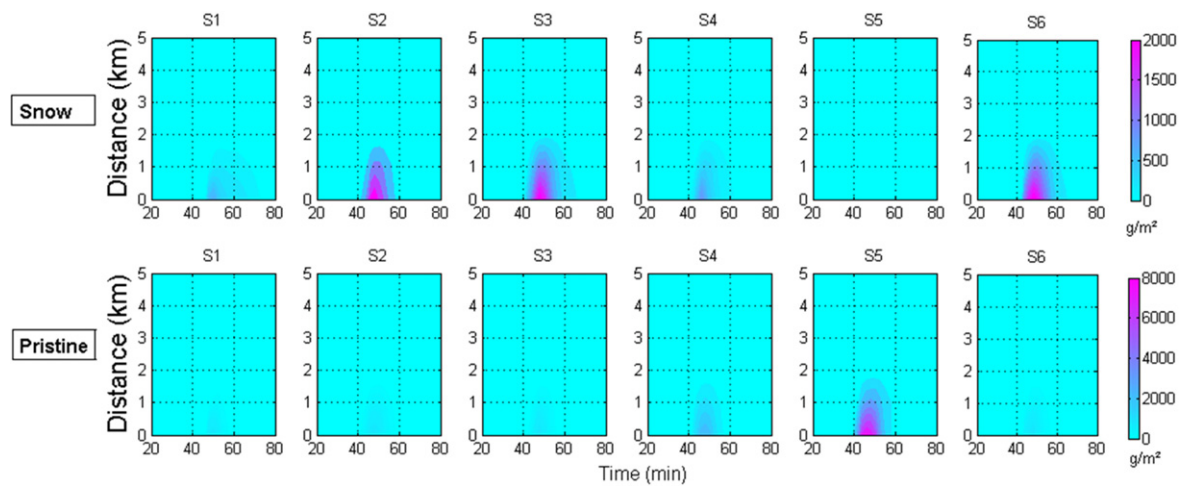


**Figure 3** Ice water path of snow and pristine crystals from BRAMS model for each simulated scenario. The vertical scale represents the horizontal extension of the cloud from its center and the horizontal scale indicates the time evolution of the cloud.

snow prevails in the bacterial scenarios (S2, S3, S4 and S6). S1 presents low concentrations of ice crystals, as expected due to its dependency only on homogeneous nucleation. Given the discussion on average particle effective radius and the prevailing hydrometeor class for the analyzed scenarios, it is clear why S5 is the most optically active in the shortwave spectrum. Pristine crystals are the predominant hydrometeor class for S5, which exhibits the smallest mean effective radius. The simulation considering the BRAMS default plus bacterial ice nucleation (S6) stimulated the production of snow and aggregates rather than pristine ice, which explains its reduced reflectivity compared to S5.

In order to illustrate the differences in cloud extent and lifetime among the scenarios, figure 4 was generated. It exhibits the time interval and extent to which pristine ice particles produced a cloud with optical depth greater than 0.7. It can be seen that by adding bacteria and considering this the only nucleation process in addition to homogeneous nucleation, the cloud lasts longer and has greater spatial extent. However, when comparing S6 to the BRAMS default, the cloud showed reduced lifetime and extent, owing to the action of other ice nucleation mechanisms besides ice nucleation due to bacteria.

Upward and downward irradiances at the top of the atmosphere and at the surface are shown in table 3 (short-wave) and table 4 (longwave), averaged over the same domain used for table 2. The relative differences are also displayed, taking the BRAMS default simulation (S5) as a reference. In the shortwave spectrum (table 3) the largest upward irradiance at the top of the atmosphere is predicted for S5 ( $529.6 \text{ W m}^{-2}$ ), whereas the inverse occurs for downward shortwave irradiance at the surface ( $390.6 \text{ W m}^{-2}$ ). These respective quantities for S6 were 14% lower and 15% larger when compared to S5. This is partially due to the differences in cloud lifetime and spatial extent and also due to an enhanced optical activity in S5, fostered by the predominance of smaller hydrometeor sizes. If we regard only the simulations considering homogeneous and bacterial ice nucleation

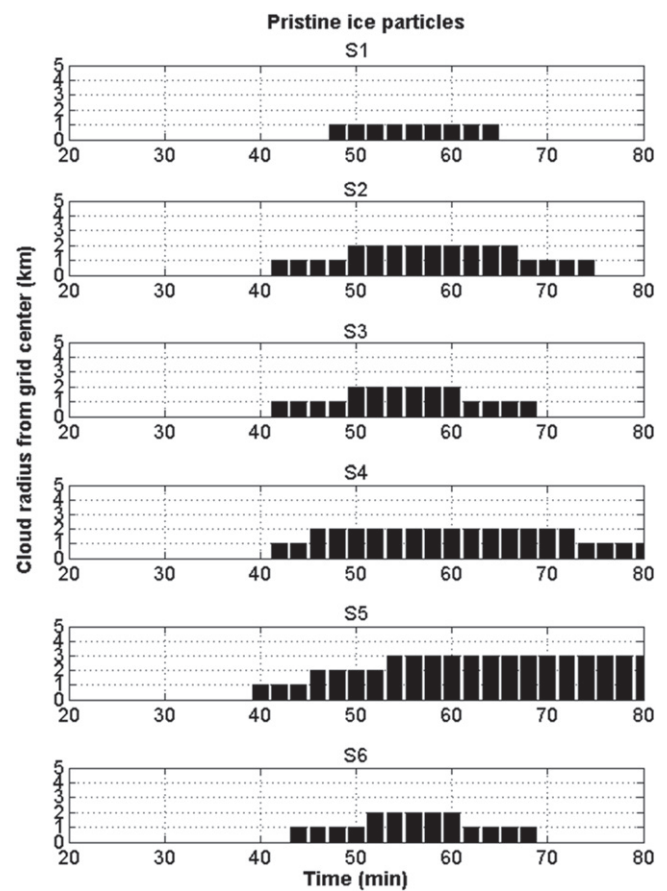


**Figure 4** Spatial extension and time length of the pristine ice part of the cell for each scenario.

(S2, S3 and S4), optical activity is enhanced with the inclusion of bacterial IN when compared to S1. In this case the largest difference was found between S4 and S1,  $21 \text{ W m}^{-2}$  (approximately 5%) for upward irradiance at the top of the atmosphere, and  $-20 \text{ W m}^{-2}$  (approximately -4%) of downward irradiance at the surface.

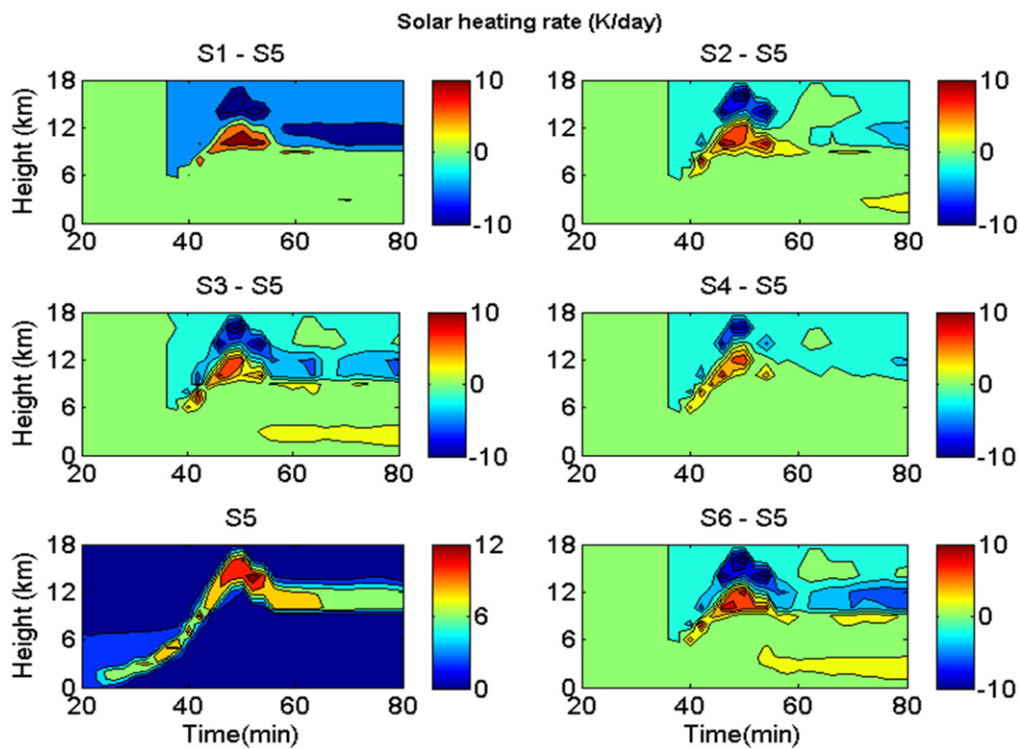


**Figure 5** Time evolution of solar heating rate for scenario S5 and relative differences of solar heating rate for the remaining scenarios, taking S5 as reference. Values observed in the cell center.

**Table 3.** Shortwave upward and downward irradiance at the top of the atmosphere and at the surface. Values were averaged over a domain of 5 km within the cell center and from 20 to 80 min of the simulations. The relative differences (%) compared to the BRAMS default are shown in parentheses.

	Shortwave irradiance ( $\text{W m}^{-2}$ )					
	S1	S2	S3	S4	S5	S6
TOA upwards	456.0	465.2 (2.0%)	462.5 (1.4%)	477.5 (4.7%)	529.6	455.6 (-14%)
z	-3.2	-2.8	-2.9	-2.2	0.0	-3.2
SFC downwards	449.6	439.8 (-2.2%)	441.1 (-1.9%)	429.7 (-4.4%)	390.6	450.3 (15%)
z	1.9	1.6	1.7	1.3	0.0	2.0

**Table 4.** Longwave upward and downward irradiance at the top of the atmosphere and at the surface. Values were averaged over a domain of 5 km within the cell center and from 20 to 80 min of the simulations. The relative differences (%) compared to the BRAMS default are shown in parentheses.

	Longwave irradiance ( $\text{W m}^{-2}$ )					
	S1	S2	S3	S4	S5	S6
TOA upwards	239.3 (16%)	221.1 (7%)	223.8 (8%)	218.1 (6%)	206.6	227.9 (10%)
z	5.1	2.0	2.5	1.6	0.0	3.1
SFC downwards	415.1 (0%)	415.1 (0%)	415.1 (0%)	415.1 (0%)	415.2	415.1 (0%)
z	0.0	0.0	0.0	0.0	0.0	0.0

In the thermal infrared spectrum, in contrast to water clouds, ice clouds can behave as gray bodies, i.e. its emissivity may be lower than unity. Moreover, since the absorption and scattering coefficients are greater for smaller ice particles, less radiation escapes the atmosphere under this situation. Table 4 shows that the averaged longwave emission is smallest in the simulation S5. This fact may be attributed both to the increased cloud lifetime and spatial extent for this

scenario, as well as to its smaller ice particle size. The upward emission for S6 was 10% larger than in S5. Likewise, S1, S2, S3 and S4 scenarios exhibited increased emission in comparison to S5: 16%, 7%, 8%, and 6%, respectively, again as a result of the differences in cloud lifetime and spatial extent. Figure 2 shows the upward longwave irradiance at TOA and illustrates these results. At the surface, no appreciable differences among the scenarios were observed, what is

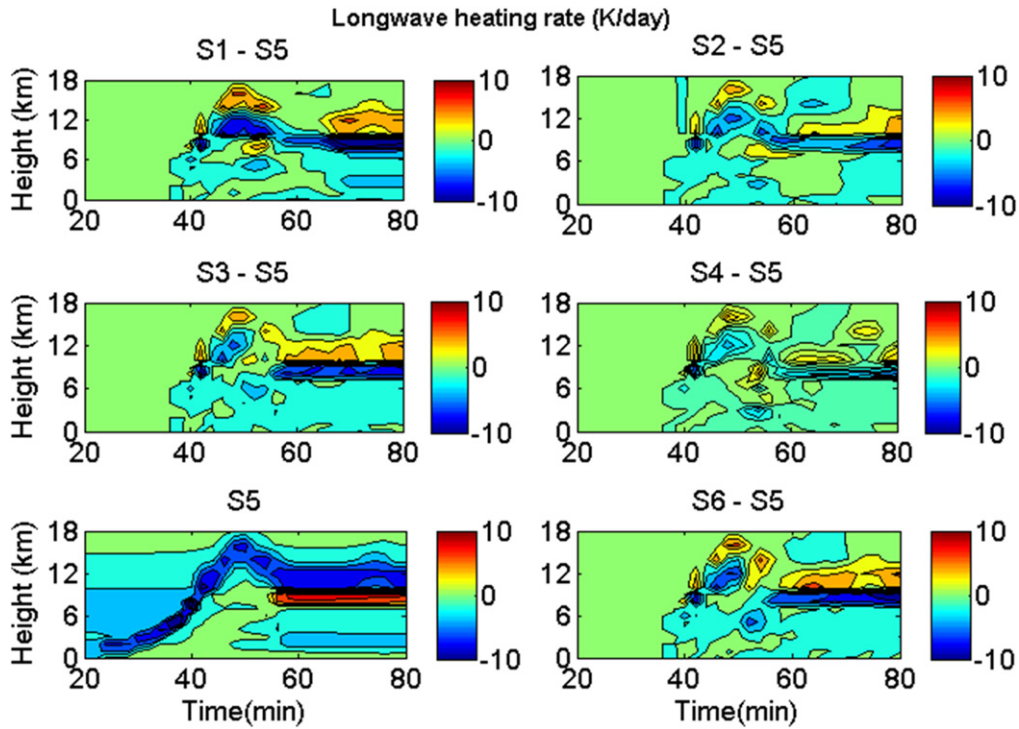


**Figure 6** Time evolution of longwave heating rate for scenario S5 and relative differences of solar heating rate for the remaining scenarios, taking S5 as reference. Values observed in the cell center.

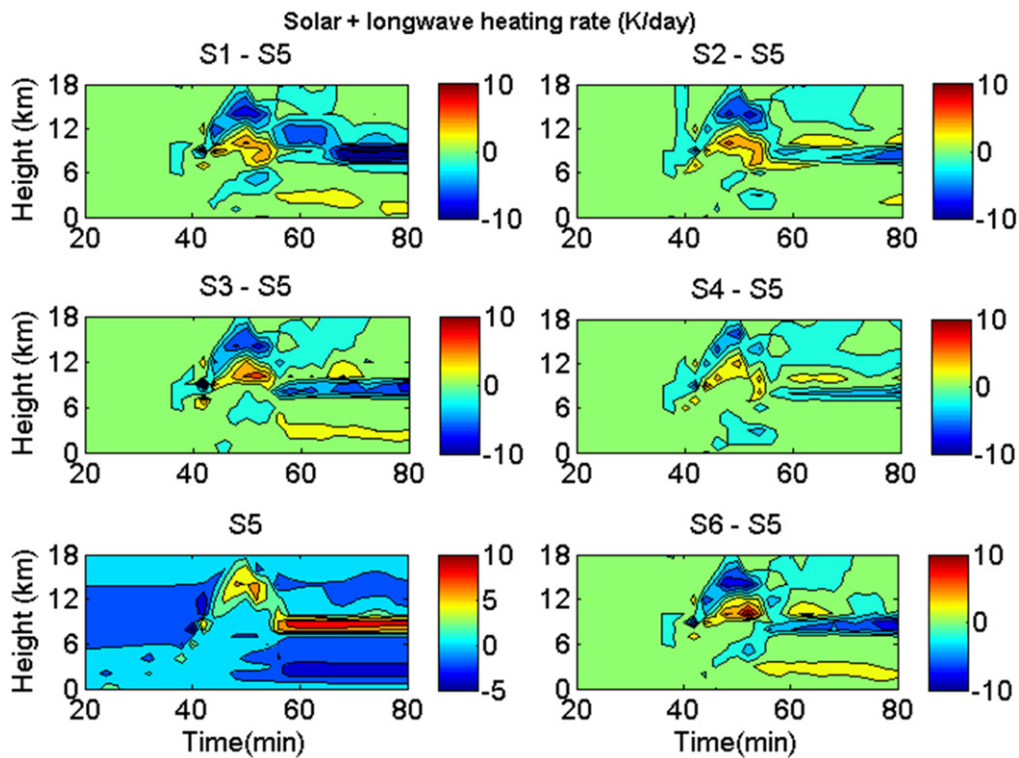


**Figure 7** Time evolution of solar and longwave heating rate for scenario S5 and relative differences of solar heating rate for the remaining scenarios, taking S5 as reference. Values observed in the cell center.

attributed to the presence of blackbody water clouds in the lower atmosphere. Although the temperature profiles can potentially affect the longwave emission, the differences among scenarios were negligible on average.

Figures 5–7 illustrate the time evolution of radiative heating/cooling rates in the shortwave (figure 5), longwave (figure 6), and total (both spectra combined, figure 7) in the cell center. In the shortwave spectrum, the differences are

related to the distinct lifetimes and also to the microphysical properties of the ice hydrometeors, given that reduced effective radius increases scattering efficiency by cloud particles. In the longwave spectrum, cloud lifetime plays a major role in the observed differences, although the cloud top height and base are also of strong relevance. In this spectral region, the patterns of cooling at cloud top and heating at cloud base are extended in time with the inclusion of bacterial IN (S2, S3 and S4) when compared to S1, but shortened when comparing S6 to S5.

#### 4. Conclusions

Numerical experiments using BRAMS were employed in order to investigate the sensitivity of properties of a convective cloud to the concentrations of bacterial IN. The simulations reproduced a convective cell over São Paulo. Changes in cloud microphysical parameters, lifetime, and spatial extent were then examined in the context of their local radiative impact.

Spatiotemporal averages over 5 km within the cell center and from 20 thru 80 min of the simulations revealed enhanced shortwave reflection at the top of the atmosphere associated with bacterial load (S2, S3 and S4) when compared to S1, with a maximum difference of approximately  $21 \text{ W m}^{-2}$  (or 5%) (S4–S1). At the surface, a reduction of  $20 \text{ W m}^{-2}$  (or 4%) in the downward shortwave irradiance was observed. In the longwave spectrum a decrease in upward irradiance at the top of the atmosphere was noticed, with a maximum difference of approximately  $21 \text{ W m}^{-2}$  (or 9%) (S4–S1). At the surface, on the other hand, no significant differences in the downward longwave irradiance were detected. These results are mainly linked with a noted increment in cloud lifetime and spatial extent correlated with increased bacterial concentration. Furthermore, in the shortwave spectrum the results are associated with a substantial reduction in the effective radius of ice hydrometers, which increased cloud reflectivity.

Large contrasts were found between radiative properties derived from the default BRAMS (S5) and from the parameterization that considers the default BRAMS plus ice nucleation due to bacteria (S6). Average values showed that, in the shortwave spectrum, the inclusion of bacterial IN induced a decrease of  $74 \text{ W m}^{-2}$  (or 14%) in the upward irradiance at the top of the atmosphere when compared to S5, whereas at the surface the incoming shortwave irradiance increased in  $60 \text{ W m}^{-2}$  (or 15%). In the longwave spectrum, the upward irradiance increased by  $21 \text{ W m}^{-2}$  (or 10%) at the top of the atmosphere when comparing S6 to S5, with no appreciable difference in the downward irradiance at the surface.

The insertion of ice nucleation due to bacteria such as *P. syringae* in a numerical model was shown to potentially influence the evolution of a convective cloud and its microphysical properties. As a consequence, the local radiative budget and heating rates have also exhibited appreciable modifications, which in turn can also affect cloud evolution by virtue of changes in thermodynamic stability. These results

suggest that, under moderate to high concentrations of bacterial aerosols, omission of bacterial IN in numerical models, as well as global cloud models, may neglect relevant ice nucleation activities at temperatures warmer than  $-8^\circ\text{C}$ , a temperature range of ice nucleation associated with particles of biological origin in the atmosphere.

#### References

- Bigg E K 1973 Ice nucleus concentrations in remote areas *J. Atmos. Sci.* **30** 1153–7
- Cotton W R *et al* 2003 RAMS 2001: current status and future directions *Meteorol. Atmos. Phys.* **82** 5–29
- Cotton W R, Tripoli G J, Rauber R M and Mulvihill E A 1986 Numerical simulation of the effects of varying ice crystal nucleation rates and aggregation processes on orographic snowfall *J. Climate Appl. Meteorol.* **25** 1668–80
- DeMott P J, Meyers M P and Cotton W R 1994 Parameterization and impact of ice initiation 755 processes relevant to numerical model simulations of cirrus clouds *J. Atmos. Sci.* **51** 77–90
- Flatau P, Tripoli G, Verlinde J and Cotton W 1989 The CSU-RAMS cloud microphysics module: general theory and code documentation Paper no. 451 Colorado State University
- Forster P *et al* 2007 Changes in Atmospheric Constituents and in Radiative Forcing *Climate Change 2007: The Physical Science Basis. Contribution of Working Group I to the Fourth Assessment Report of the Intergovernmental Panel on Climate Change* ed S Solomon, D Qin, M Manning, Z Chen, M Marquis, K B Averyt, M Tignor and H L Miller (Cambridge, UK: Cambridge University Press) pp 747–845
- Fu Q and Liou K 1992 On the correlated k-distribution method for radiative transfer in nonhomogeneous atmospheres *J. Atmos. Sci.* **49** 2139–56
- Gonçalves F L T, Martins J A, Albrecht R I, Morales C A, Silva Dias M A F and Morris C E 2012 Effect of bacterial ice nuclei on the frequency and intensity of lightning activity inferred by the BRAMS model *Atmos. Chem. Phys.* **12** 5677–89
- Gonçalves F L T, Martins J A and Silva Dias M A F 2008 Shape parameter analysis using cloud spectra and gamma functions in the numerical modeling RAMS during LBA project at amazonian region, Brazil *Atmos. Res.* **89** 1–11
- Hallett J and Mossop S C 1974 Production of secondary ice particles during riming process *Nature* **249** 26–8
- Hoose C, Kristjánsson J E and Burrows S 2010 How important is biological ice nucleation in clouds on a global scale? *Environ. Res. Lett.* **5** 024009
- Hu Y X and Stamnes K 1993 An accurate parameterization of the radiative properties of water clouds suitable for use in climate models *J. Clim.* **6** 728–42
- Kato S, Ackerman T P, Mather J H and Clothiaux E 1999 The k-distribution method and correlated-k approximation for a shortwave radiative transfer model *J. Quant. Spectrosc. Radiat. Transfer* **62** 109–21
- Khain A P, Ovtchinnikov M, Pinsky M, Pokrovsky A and Krugliak H 2000 Notes on the state-of-the art numerical modeling of cloud microphysics *Atmos. Res.* **55** 159–224
- Knopf D A, Alpert P A, Wang B and Aller J Y 2011 Stimulation of ice nucleation by marine diatoms *Nat. Geosci.* **4** 88–90
- Kylling A, Stamnes K and Tsay S C 1995 A reliable and efficient two-stream algorithm for spherical radiative transfer: Documentation of accuracy in realistic layered media *J. Atmos. Chem.* **21** 115–50
- Loveland T and Belward A 1997 The IGBP-DIS global 1 km land cover data set, DISCover: first results. international *J. Remote Sens.* **18** 3289–95

- Mayer B and Kylling A 2005 Technical note: the libRadtran software package for radiative transfer calculations—description and examples of use *Atmos. Chem. Phys.* **5** 1855–77
- Meyers M P, Demott P J and Cotton W R 1992 New primary ice-nucleation parameterizations in an explicit cloud model *J. Appl. Meteor.* **31** 708–21
- Meyers M P, Walko R L, Harrington J Y and Cotton W R 1997 New RAMS cloud microphysics parameterization. part II: the two-moment scheme *Atmos. Res.* **45** 3–39
- Morris C E, Conen F, Huffman J A, Phillips V, Poeschl U and Sands D C 2014 Bioprecipitation: a feedback cycle linking Earth history, ecosystem dynamics and land use through biological ice nucleators in the atmosphere. *Glob. Change Biol.* **20** 341–51
- Morris C E, Sands D C, Bardin M, Jaenicke R, Vogel B, Leyronas C, Ariya P A and Psenner R 2011 Microbiology and atmospheric processes: research challenges concerning the impact of airborne micro-organisms on the atmosphere and climate *Biogeosciences* **8** 17–25
- Mossop S C 1976 Production of secondary ice particles during the growth of graupel by riming *Q. J. R. Meteorol. Soc.* **102** 45–57
- Pielke R A *et al* 1992 A comprehensive meteorological modeling system—RAMS *Meteorol. Atmos. Phys.* **49** 69–91
- Pratt K A, DeMott P J, French J R, Wang Z, Westphal D L, Heymsfield A J, Twohy C H, Prenni A J and Prather K A 2009 *In situ* detection of biological particles in cloud ice-crystals *Nat. Geosci.* **2** 398–401
- Prenni A J, Petters M D, Kreidenweis S M, Heald C L, Martin S T, Artaxo P, Garland R M, Wollny A G and Pöschl U 2009 Relative roles of biogenic emissions and saharan dust as ice nuclei in the Amazon basin *Nat. Geosci.* **2** 401–4
- Sesartic A, Lohmann U and Storelvmo T 2012 Bacteria in the ECHAM5-HAM global climate model *Atmos. Chem. Phys.* **12** 8645–61
- Spracklen D V and Heald C L 2013 The contribution of fungal spores and bacteria to regional and global aerosol number and ice nucleation immersion freezing rates *Atmos. Chem. Phys. Discuss.* **13** 32459–81
- Twomey S and Wojciechowski T A 1969 Observations of the geographical variation of the cloud nuclei *J. Atmos. Sci.* **26** 684–8
- Väitilingom M, Deguillaume L, Vinatier V, Sancelme M, Amato P, Chaumerliac N and Delort A M 2013 Potential impact of microbial activity on the oxidant capacity and organic carbon budget in clouds *Proc. Natl. Acad. Sci.* **110** 559–64
- Walko R, Cotton W R, Meyers M P and Harrington J Y 1995 New RAMS cloud microphysics parameterization. part I: the single-moment scheme *Atmos. Res.* **38** 29–62
- Wilks D 2006 *Statistical Methods in Atmospheric Sciences* (San Diego, CA: Academic)
- Yang P, Wei H, Huang H L, Baum B A, Hu Y X, Kattawar G W, Mishchenko M I and Fu Q 2005 Scattering and absorption property database for nonspherical ice particles in the near-through far-infrared spectral region *Appl. Opt.* **44** 5512–23
- Yun Y and Penner J E 2013 An evaluation of the potential radiative forcing and climatic impact of marine organic aerosols as heterogeneous ice nuclei *Geophys. Res. Lett.* **40** 4121–6